Structural characterization and chemistry of LiF–AlF3 melts with addition of MgO and MgF2

Aydar Rakhmatullin, Rudy Michel, Catherine Bessada

Structural characterization and chemistry of $LiF-AlF_3$ melts with addition of MgO and MgF_2

Aydar Rakhmatullin*, Rudy Michel, and Catherine Bessada

Conditions Extrémes et Matériaux: Haute Temperature et Irradiation CNRS, 1D av. de la Recherche Scientifique, 450 71 Orléans, France

**Corresponding authors*: Aydar Rakhmatullin, e-mail: rakhmat@cnrs-orleans.fr, tel.: 0033-238255512

Abstract

The $LiF-AlF_3$ system with additions of MgO and MgF_2 has been studied by ^{17}O, ^{25}Mg, ^{27}Al and ^{19}F *in-situ* high temperature NMR, *ex-situ* solid state NMR and X-ray powder diffraction for a wide range of compositions. The description of the speciation in the melts and its evolution with different operational parameters such as temperature, time and composition were obtained for MgF_2/MgO-(1-*x*)LiF-*x*AlF_3 for *x*=14.5, 25 and 35.5 mol% systems. The evolution of the signals provides evidence of a chemical reaction between the MgO and the salt.

Keywords: system MgO/MgF_2-LiF-*x*AlF_3, molten salts, high temperature and solid state NMR, nuclear reactors

1. Introduction

Numerous study and research projects have been conducted on the targets in the core of an SFR (sodium cooled nuclear reactors) (for example, see [1, 2]). One of the main questions is to know if the potential extraction step of americium in $LiF-AlF_3$ can be used with a CERCER (ceramic-ceramic) targets containing MgO matrix retreatment [1, 3, 4]. This process, known as liquid-liquid reductive extraction, consists of a molten metallic aluminum pool in contact with Am ions in the molten salt. The metals will be extracted from one phase to the other.

The phase diagram of the $LiF-AlF_3$ system has been studied by several authors [5-7]. A compound Li_3AlF_6 as well as two eutectics at 14.5 and 35.5 mol% AlF_3 have been reported. The $MgF_2-Li_3AlF_6$ pseudo-binary is a eutectic system. According to Kasicova *et al.* [8], eutectic point is located at 37 mol% MgF_2 and 63 mol% Li_3AlF_6, with t_{eut} =748 °C, but up to now, no more details were collected on this system. In the literature, many studies were reported on the $MgF_2-Na_3AlF_6$ system, because of its big interest in aluminium electrolysis. Several investigations [9-11] of the $MgF_2-Na_3AlF_6$ phase diagram have been published. Kostyukov and Karpov [11] have reported that this system does not form a simple binary system. By cooling a molten mixture with a low content of magnesium fluoride, the solid compound $NaMgF_3$ precipitates:

$$Na_3AlF_6 + 3MgF_2 \rightarrow AlF_3 + 3NaMgF_3 \quad (1)$$

At higher MgF_2 contents, the incongruently melting compound Na_2MgAlF_7 is formed, and presumably also $Na_2Mg_2Al_3F_{15}$. MgF_2 forms a solid solution with sodium cryolite, the composition of which may be taken from their phase diagram [11]. The same feature was also

supported by Holm [10] on the basis of thermal, X-ray and optical analysis of mixtures containing more than 75 mol% cryolite. Sokolov *et al.* [11] and Kostyukov *et al.* [12] assumed that magnesium fluoride is present in sodium cryolite-based melts as MgF_3^- anions. They suppose that the formation of these complex anions influences on the activity of aluminium complexes in the melt. In the reference [13] authors built different structural models for the MgF_2 dissolution in molten sodium cryolite. Their calculated results indicate that the presence of MgF_4^{2-} ions is more probable than MgF_3^- or Mg^{2+}. The *in-situ* high temperature (HT) Raman spectroscopic study of the MgF_2–Na_3AlF_6 system was carried out by Gilbert *et al.* [14]. From their analysis, MgF_2 is an acidic additive and tends to form MgF_3^- or MgF_4^{2-} species. $Mg_2F_6^{2-}$ is always a minor species compared to the tetrahedral complex MgF_4^{2-}. They have also reported the formation of a bridged complex, such as $Mg_2F_6^{2-}$, for high amount of MgF_2.

Compare with the MgF_2–Na_3AlF_6 system only a few studies have been made in MgO–Na_3AlF_6. An eutectic was found at approximately 30 mol% and 892 °C [15]. According to Kostyukov *et al.* [12] MgO reacts rapidly with aluminium fluoride and forms magnesium fluoride and alumina.

High temperature NMR spectroscopy can provide an experimental description of different species existing in melts. This method is sensitive to the first coordination sphere around a given cation. Because of the aggressivity and reactivity of molten fluorides at high temperature, their experimental characterization is difficult and only a few spectroscopies (Raman [16, 14], NMR [16-19], and extended X-ray absorption fine structure (EXAFS) [17]) were able to extend the description of such systems.

Therefore, the aim of present study is focused on the fundamental description of the system LiF–AlF_3 melts with addition of MgF_2 and MgO. We have first performed high

temperature NMR (HT NMR) experiments on $LiF-AlF_3$ melts with different additions of MgF_2 and MgO in order to follow the modification of aluminium first coordination shell upon fluoride and oxide addition. In a second step, we used solid-state NMR and X-ray diffraction to identify and further characterize the samples after HT NMR experiments. The combination of these techniques has proved to be a powerful tool in elucidating the structure in complex crystalline and/or disordered materials.

2. Results and Discussion

2.1. MgF_2 additions in molten $LiF-AlF_3$ mixtures

2.1.1. High temperature NMR results

In the melt, the HT NMR spectra consist in a single Lorentzian line, characteristic of a rapid exchange between the different species. The measured chemical shift is the weighted average of the individual chemical shifts of all species present in the melt [18]. From the knowledge of the individual chemical shifts of the different species present in the melt, it is thus possible to extract the distribution the different ionic configurations depending on the composition.

2.1.1.1. 85.5-14.5 mol% $LiF-AlF_3$ + MgF_2 and 75-25 mol% $LiF-AlF_3$ + MgF_2

We have followed the effect of MgF_2 additions in the two $LiF-AlF_3$ mixtures: 14.5 and 25 mol% AlF_3 at 3 different temperatures in the melt (see Table 1).

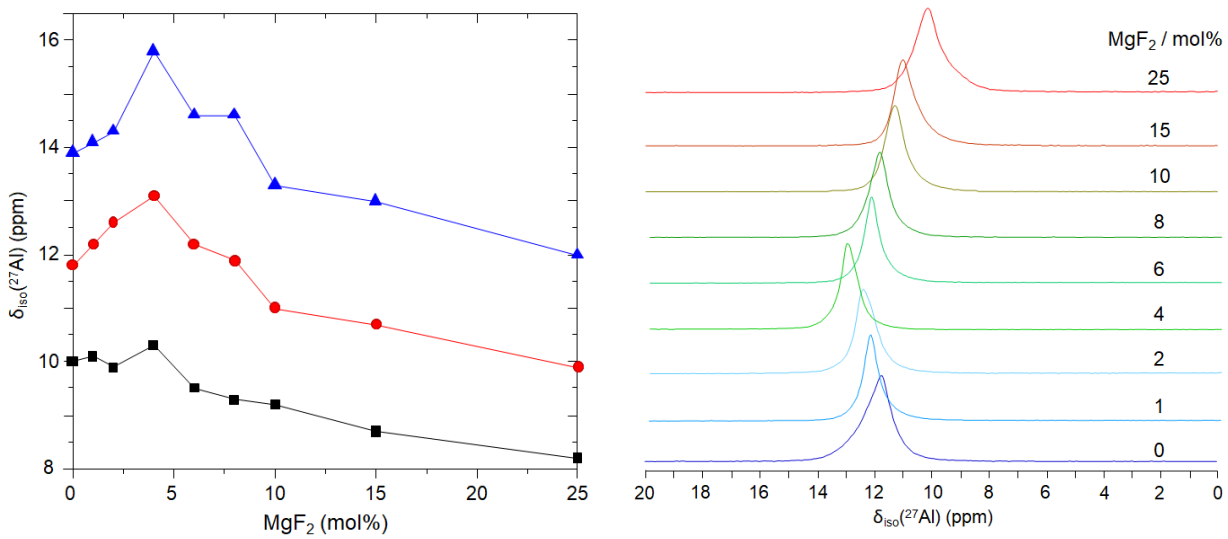

Fig. 1. On the left: evolution of ^{27}Al chemical shifts for different addition of MgF_2 (0 to 25 mol%) in molten Li_3AlF_6 at ■ 800, ● 880, and ▲ 960 °C. On the right: The ^{27}Al NMR spectra of Li_3AlF_6–MgF_2 mixtures at 880 °C.

In the system Li_3AlF_6–MgF_2 we observe a clear variation of the ^{27}Al chemical shifts (the position of the line) with a maximum observed between 4 and 6 mol% MgF_2. We have reported in the Fig. 1 the ^{27}Al chemical shifts measured in pure molten Li_3AlF_6 at 800, 880 and 900 °C. We notice the effect of temperature with a systematic shift of 2 ppm/80 °C for each composition. While the effect of composition (mol% MgF_2) is visible by the particular evolution of the chemical shifts: an increase up to a maximum value at around 5 mol% MgF_2 and then a decrease. In order to go further we have compared these data with the information given by the other nuclei ^{19}F and ^{25}Mg. Even if ^{7}Li is observable by NMR and present in the sample, the chemical shifts range of diamagnetic lithium is too small to be informative. We don't observe any variation of the ^{19}F signal position with MgF_2 addition, which stays at -183 ppm at 880 °C as in the pure Li_3AlF_6

without MgF_2. We just mention a shift of -2 ppm with temperature between 800 and 960 °C for all compositions.

The ^{25}Mg signal is not influenced by the amount of MgF_2 and appears at the same position (±1 ppm) than in pure molten MgF_2 *i.e.* at -4.1 ppm in this range of composition. The resolution of the spectra is poor, but good enough to determine the position. Nevertheless it is difficult to obtain the ^{25}Mg NMR signal with good signal-to-noise ratio for MgF_2 additions less than 10 % due to low natural abundance (10%) and small gyromagnetic ratio of magnesium nucleus [20]. If we consider the phase diagram of this system, over this range of MgF_2 addition, no specific feature is observed for the concentration of MgF_2 below 5 mol%. The evolution observed for ^{27}Al chemical shifts can be attributed to a slight change on speciation in the melt. This change does not seem to influence the fluorine and magnesium signals.

In the system 85.5-14.5 mol% $LiF{-}AlF_3$ + MgF_2 the changes in the ^{27}Al signal position with MgF_2 addition were less noticeable. We have observed ±1ppm chemical shift variation with MgF_2 additions and we notice the effect of temperature with a systematic shift of 1.5 ppm/80°C for each composition.

2.1.1.2. 64.5-35.5 mol% $LiF{-}AlF_3$ + MgF_2

We performed *in-situ* NMR measurements at high temperature for 2, 4, 6, 8, 10, 15 mol% MgF_2 additions but we obtained a good Lorentzian line shape signal of "pure liquid" only for small concentrations of magnesium fluoride: 2 and 4 mol%. For higher concentrations ^{27}Al and ^{19}F spectra were rather complex with different peaks corresponding to a mixture of solid and liquid

phases. The system is not stable, even just above the liquidus temperatures with strong sublimation phenomena and rapid evolution of the bath chemistry.

2.1.2. X-ray results

After the HT NMR experiments the solidified ternary mixtures were systematically characterized by X-Rays diffraction at room temperature. In case of MgF_2 for the concentrations up to 25 mol% we observe the presence of MgF_2, AlF_3 and as well as expected Li_3AlF_6. At high contents of MgF_2, in addition with Li_3AlF_6, MgF_2 and AlF_3, the formation of a new phase $LiMgAlF_6$ [21] was detected.

2.2. MgO additions in molten LiF−AlF_3 mixtures

2.2.1. High temperature NMR results

Thanks to the information given by ^{27}Al, ^{25}Mg, ^{19}F and ^{17}O we describe the effect of MgO additions in the melts i.e. with three different AlF_3 contents. The NMR data were collected at 800 °C, 880 °C and 960 °C for 14.5 mol% and 25 mol% AlF_3.

For 35.5 mol% AlF_3 we obtained a good sharp signal corresponding to the melt at 900°C. For the lower temperature, we observed the signals corresponding to a mixture of solid and liquid phases. For the temperatures higher that 900 °C, after about 10 minutes we have found new broad "solid" signal with full width at half maximum of few kHz due to strong sublimation phenomena.

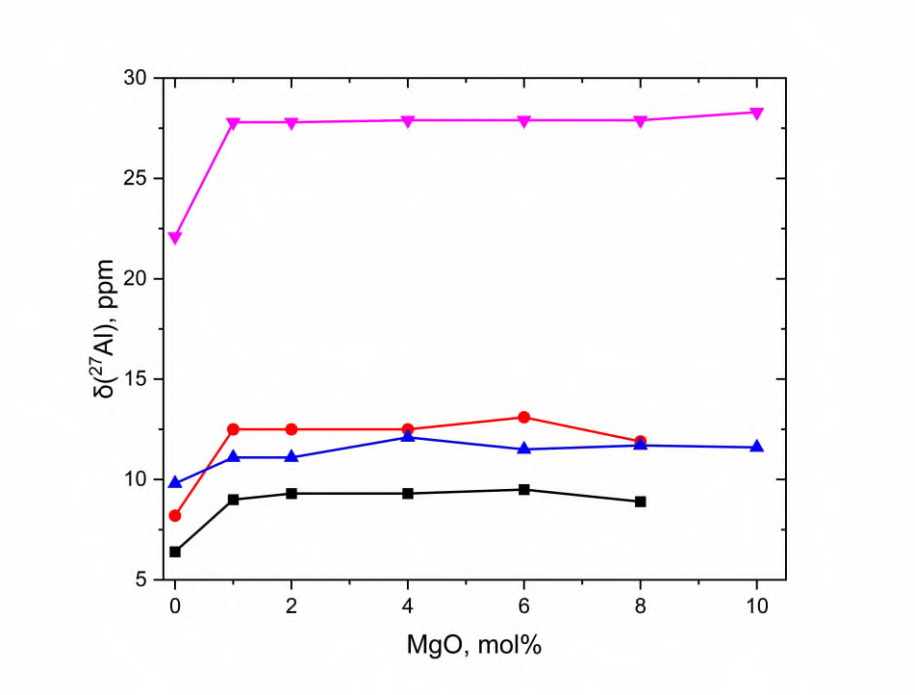

Fig. 2. ^{27}Al chemical shifts for different addition of MgO (0 to 10 mol%) measured in the mixtures with 14.5 mol% AlF_3 (■ 800 °C, ● 900 °C), 25 mol% (▲ 800 °C), and 35.5 mol% (▼ 900 °C).

We have reported on Fig. 2 the ^{27}Al chemical shifts measured in the systems with MgO additions. We observed for all systems, that the only visible modification occurring with the addition of MgO up to 1 mol% with a systematic increase of the chemical shift value. The chemical shifts are remaining constant for higher than 1 mol% MgO content. The range of chemical shifts, where the variation is discussed, is quite small 2-3 ppm, and it indicates that if modification occurs in the melt, it doesn't affect strongly the local environment of the aluminum.

The ^{17}O signal is detected in the melt even at very low MgO content. In all systems its position remains constant and only the intensity of the peak is varying, corresponding to more oxygen in the liquid phase. In the system with 14.5 mol% AlF_3 the position is (38±1) ppm, while for highest

AlF_3 content 25 mol% and 35.5 mol% the position is at (30±1) ppm and (26.7±0.5) ppm respectively, and with no influence of the temperature.

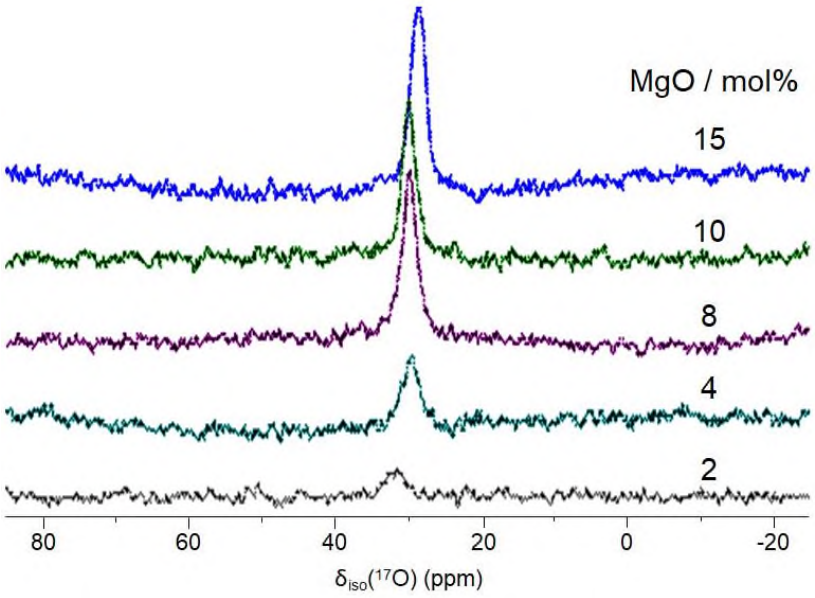

Fig. 3. ^{17}O NMR spectra in Li_3AlF_6 with different MgO additions (from 2 to 15 mol%). The ^{17}O spectra were collected just above the melting point.

We notice also that the magnesium oxide is solubilized in the bath, the ^{17}O signal intensities increase with MgO additions (Fig. 3).

The ^{25}Mg signal is slightly influenced by the amount of MgO compare with pure molten MgF_2 *i.e.* at -4.1 ppm. It appears at (-7.0±1) ppm in this range of composition. The spectral signal to noise ratio is low, but enough is retained to provide a reasonably accurate measurement of the position. Nevertheless, it is difficult to obtain the signal for MgO additions less than 10 mol%. It should be noted that in the system MgO−Li_3AlF_6 a small effect of temperature was observed, the chemical shifts increase slightly (+1 ppm) for the changing of the temperature from 800 °C to 960 °C.

2.2.2. X-ray results

The X-ray pattern of samples, with 14.5 and 25 mol% AlF_3 contains the lines of precursor LiF, Li_3AlF_6 and two new phases, namely magnesium fluoride and alumina. Some traces of BN powder are due to the crucible were observed. For the 35.5 mol% AlF_3, we also detected $LiMgAlF_6$ [21].

2.2.3. Solid state NMR

Solid state ^{27}Al NMR spectra of the same solidified mixtures show 3 signals, one very broad signal with maximum at around 65 ppm from aluminium in tetrahedral and two intense symmetric lines at -2 ppm and -16 ppm with spinning sidebands associated with a relatively low quadrupolar interaction from aluminium in octahedral coordination, which can be attributed to the lithium cryolite and aluminium fluoride. Transition alumina phases contain aluminium ions in two different types of tetrahedral, signals with maximum at 65 ppm, and octahedral coordination which covered by intense cryolite signal [22].

The ^{17}O NMR spectra show two overlapping resonances near 40 ppm and 60 ppm. Simulation of these spectra as the sum of two broad Gaussian line shapes with full width at half maximum (FWHM) ca. 3700 and 2400 Hz as illustrated in Fig. 4, presumably due to a broad distribution of quadrupole coupling parameters. We indicate that the ratio of the integrated intensities of the two resonances is approximately 1:1. The same distribution of the aluminium sites was founded for different alumina phases by Walter and Oldfield [23]. We assign the narrower resonance at 40 ppm to the OAl_3 sites and the broader peak at 60 ppm to the trigonal

OAl_4 sites. The greater breadth of this latter resonance is attributed to a larger quadrupole coupling constant for these tetrahedral sites, although we cannot discern any second-order quadrupolar splitting in the line shape. NMR results are in good agreement with the XRD data.

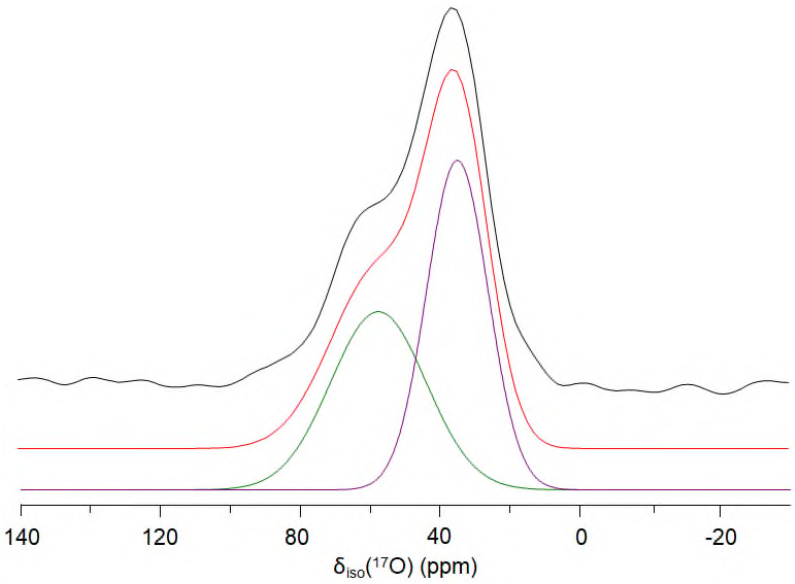

Fig. 4. ^{17}O MAS NMR experimental (black line) spectrum and it simulation (color lines) of Li_3AlF_6 with 6 mol% MgO solidified mixture.

Lacassagne *et al.* [18] reported the ^{19}F chemical shift values for AlF_6^{3-}, AlF_5^{2-} and AlF_4^- at δ = -176 ppm, δ = -188 ppm, and δ = -200 ppm respectively. For the pure molten LiF, $\delta(^{19}F)$= -201 ppm is assigned to the free fluorine ion. In our measurements ^{19}F chemical shifts slight decrease with MgF and MgO content over the whole range of compositions from -182 to -186 ppm and consequently fluorine atoms are involved in all AlF_6^{3-}, AlF_5^{2-} and AlF_4^- complexes, and in free fluorine ions F^-. For the all mixtures, we have observed the decrease of the fluorine chemical shifts with the temperature. It is worth noting the important contribution of AlF_5^{2-}

species in the melt and the increasing of amount of AlF_4^- and/or free fluorine ions with increasing the temperature.

Recently Moussaed [24] studied the structure and dynamics of KF−MgF_2 and LiF−MgF_2 melts over a wide range of composition and temperature by HT NMR and HT PFG NMR. ^{25}Mg and ^{19}F NMR experimental data were also compared with MD calculations. In the case of LiF-MgF_2, ^{25}Mg chemical shifts decrease from 0.5 ppm at 5 mol% MgF_2 to -5 ppm in pure MgF_2. For the KF−MgF_2 system, the ^{25}Mg chemical shift values vary from 7 ppm for 15 mol% to -5 ppm in pure MgF_2. MD calculations in agreement with HT NMR experiments provide evidence for the coexistence of the different Mg-based complexes: MgF_4^{2-}, MgF_5^{3-}, MgF_6^{4-}, MgF_7^{5-}, and MgF_8^{6-}. The average coordination for the magnesium ion in LiF−MgF_2 system is between 5.8 and 6.0. It is worth noting the important contribution of MgF_6^{4-} complexes, around 60 % of total Mg^{2+} species. The average coordination depends on the concentration and temperature of the melt. In case of KF−MgF_2 at 10 mol% MgF_2 the average coordination is 4.8 with important contribution of MgF_5^{3-} (~60 %), and it increases up to 6 with increasing MgF_2 amount.

Based on literature data [25, 24, 26, 27] we have constructed a ^{25}Mg chemical shifts scale for the different magnesium local environments: magnesium atom surrounded by 6 fluorines at around ≈ -4 ppm, MgF_5 coordination at ≈ 7 ppm, MgO_6 at ≈ 26 ppm and MgO_4 between 48-55 ppm. We see that a magnesium atom surrounded by 6 fluorines will have a very different chemical shift than a magnesium surrounded by 6 oxygens [25]. In our systems, the measured chemical shift is the range of -3.5 to 8 ppm. Our data show that it will tend to form species with a magnesium atom surrounded by 6 fluorines. For the additions of MgO, the chemical shifts, that are relative to pure molten MgF_2 (-4.1 ppm), could be the sign of the formation of MgF_5^{3-} and MgF_6^{4-}. From ^{25}Mg NMR data we can propose the presence in the melt of species in which

magnesium atoms are surrounded by fluorine in both cases MgF and MgO and we state the magnesium don't keep its oxygen environment with adding magnesia in the bath.

The X-ray diffraction patterns obtained after cooling at room temperature confirm the transformation of MgO and show evidence of the existence of Li_3AlF_6, Al_2O_3, MgF_2, and LiF. The presence of these compounds suggests the complete reaction of magnesium oxide according to the chemical equation:

$$3MgO + 2AlF_3 \rightarrow 3MgF_2 + Al_2O_3 \quad (2)$$

This interpretation is in very good agreement with data reported by Kostyukov *et al.* in the system $NaF-AlF_3-MgO$ [12].

We report on the Fig. 5, the different ^{17}O chemical shifts measured in the melt depending on the amount AlF_3. We show also for comparison, the ^{17}O chemical shift value measured in solid MgO at 47 ppm [28] (the melting temperature of MgO, t_m =2852 °C, is too high for NMR measurements).

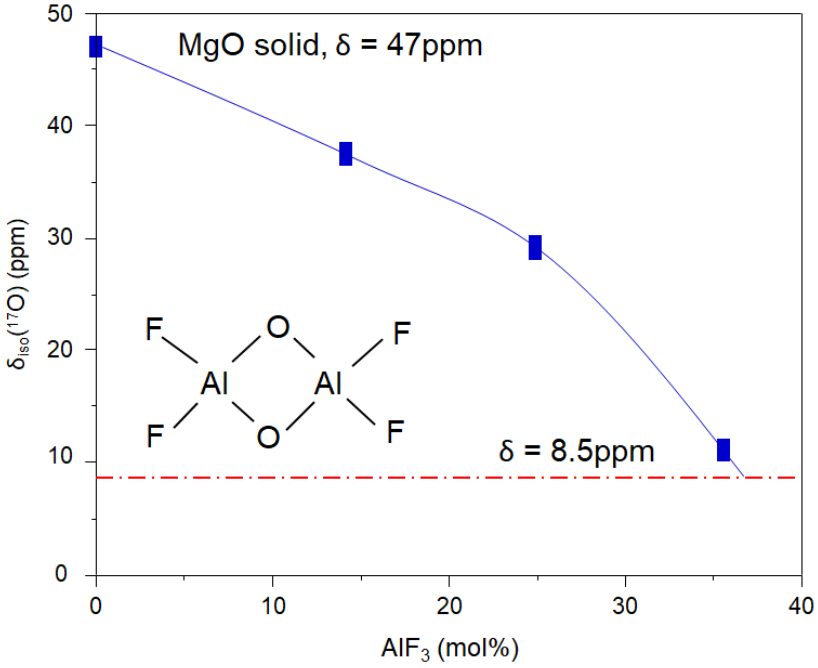

Fig. 5. Evolution of the ^{17}O chemical shift with AlF_3 composition at 900 °C.

^{17}O chemical shift value a continuous decreases from 47 ppm corresponding to an oxygen surrounded by 6 magnesium atoms [28] to 10 ppm i.e. close to the values measured for oxyfluoroaluminate anionic species, $Al_2O_2F_4^{2-}$ (8.5 ppm), where the oxygen atom is connected to 2 aluminium atoms and more precisely to 2 aluminium atoms fourfold coordinated as 2F and 2O [18].

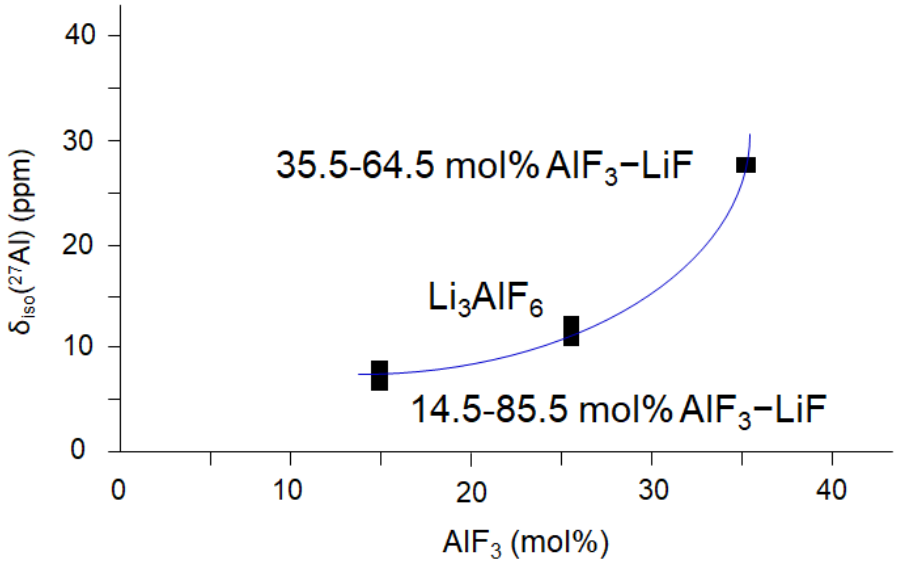

Fig. 6. The rectangles figure the ranges of ^{27}Al chemical shifts values measured for the different MgO additions at a given AlF_3 content.

These findings are confirmed by the ^{27}Al results. In pure molten initial mixtures, the fluoroaluminate species are AlF_4^-, AlF_5^{2-} and AlF_6^{3-} [16]. As we mentioned above aluminium chemical shift is remaining constant whatever the MgO content, and, consequently, the average coordination number doesn't change. However, the environment of Al changes, the fluorine atom is replaced by oxygen. On the other hand, we have observed an increase of the chemical shift values with AlF_3 content from 14.5 mol% AlF_3 at ~5 ppm up to 35.5 mol% at ~ 30 ppm, it indicates an increase of tetrahedral environments of Al (Fig. 6). The similar behavior was also observed for system NaF−AlF_3 [18, 19] : $\delta(^{27}Al) \approx 14$ ppm at 20 mol% AlF_3 and $\delta(^{27}Al) \approx 27$ ppm at 35-40 mol% AlF_3.

All our NMR measurements are consistent well with the supposition that the oxyfluoroaluminate anionic species ($Al_2O_2F_4^{2-}$) form with the additions of MgO.

From the XRD patterns recorded on the solidified mixtures of $MgO-LiF-AlF_3$, we have to note that for 35.5 mol% AlF_3 composition, we obtained after cooling a mixture involving $LiMgAlF_6$ that we had observed at high contents of MgF_2 in $MgF_2-LiF-AlF_3$. This result is in good agreement with the findings of Tao *et al.* [21], which synthesized $LiMgAlF_6$ with the excesses of MgF_2 and AlF_3 in the reaction mixture.

$LiMgF_3$ and $NaMgF_3$ are predicted to have negative enthalpies of formation from the binary fluorides -53 $kJ \times mol^{-1}$ and -30 $kJ \times mol^{-1}$ respectively [29]. But in case of $MgF_2-Na_3AlF_6$ the formation of $NaMgF_3$ as well as Na_2MgAlF_7 were observed [11]. In our work for the analogous MgF_2 containing systems we didn't observe the precipitation any others phases.

4. Conclusions

High-temperature NMR study of melts in $MgF_2-LiF-AlF_3$ and $MgO-LiF-AlF_3$ systems, by means of observation of the different nuclei involved in these systems: ^{27}Al, ^{25}Mg, ^{19}F, and ^{17}O, provides a powerful tool for the structural description of such complex liquids. In MgF_2-LiF-AlF_3 system magnesium atoms are surrounded by fluorines and the magnesium keep its sixfold coordination in the melt. The addition of MgO in the aluminium fluoride melts leads to a strong reaction with AlF_3 and to a formation of alumina. We have found a formation of a bridged complex $Al_2O_2F_4^{2-}$ in the bath, when the amount of AlF_3 increases.

5. Experimental section

5.1. Chemicals.

LiF, MgF_2 and AlF_3 were purchased from Sigma-Aldrich Co., 99.9 %. In order to detect the ^{17}O signal on MgO dissolution, because of its very low abundance (0.04 %), we have enriched the sample in ^{17}O. ^{17}O is the only isotope of the oxygen observable by NMR, because its spin is non-zero. We start from ^{17}O labeled H_2O (enrichment 40 %, CortecNet). The labeled water was added to a stoichiometric amount of magnesium ethoxide in tetrahydrofuran (THF), under dry argon. The mixture was stirred and heated for 16 hours at 55 °C. $Mg(OH)_2$ precipitated as light brown powder. Finally, solvent was distilled off and the reaction product calcined at 1400 °C for half hours. The quality of MgO was checked by X-Ray Diffraction (XRD) analysis (Bruker D8 Advance). All chemicals were handled in a glovebox with dry argon containing less than 1 ppm of water vapor.

5.2. The choice of the composition

Our approach is centered on the experimental characterization of MgO and MgF_2 additions in LiF−AlF_3 melts. Based on the LiF−AlF_3 phase diagram we propose to study the effect of the AlF_3 composition and temperature, and we focus on three compositions: eutectics 14.5 and 35.5 mol% AlF_3 with low melting temperature (707 °C) compare with the other composition, and cryolitic composition Li_3AlF_6, at 25 mol% AlF_3, with a congruent melting at 785 °C. This composition interests different other applications (aluminium electrolysis, pyrochemical treatments of nuclear wastes) and it has been extensively studied. We have then followed the effect of MgO and MgF_2 additions in the three LiF−AlF_3 mixtures: 14.5, 25, and 35.5 mol% AlF_3. The compositions of samples and the temperatures are given in Table 1.

Table 1
Compositions of the samples and temperatures of the NMR measurements.

$LiF-AlF_3$/mol%	Additives/mol%	Temperature/°C
85.5-14.5	MgF_2: 0, 4, 10	740, 820, 900
	MgO: 0, 1, 2, 4, 6, 8	800, 880, 960
75-25	MgF_2: 0, 1, 2, 4, 6, 8, 10, 15, 25	800, 880, 960
	MgO: 0, 1, 2, 4, 6, 8, 10, 15	800, 880, 960
64.5-35.5	MgF_2: 0, 2, 4, 6, 8, 10, 15	not measured
	MgO: 0, 1, 2, 4, 6, 8, 10	900

5.3. NMR measurements

The HT NMR spectra were acquired using the laser heated NMR system developed in CEMHTI Orleans [16]. The BN crucible containing the sample is placed inside the RF-coil, in the center of cryomagnet. The sample is heated by two CO_2 laser (Coherent Diamond 250W), passing axially through the NMR probe. The temperature cannot be measured inside the crucible during the spectra acquisition, so thanks to the calibration of the laser power, we can determine the temperature within ±10 °C. The melting point of the sample is clearly indicated by the modification of the shape and width of the line. The transition from solid to liquid state can be followed on ^{27}Al NMR spectra during the heating of the sample. The time "zero" corresponds to the laser power setting, the desired temperature is considered to be reached in the sample after 4-5 minutes. For example in case $MgF_2-Li_3AlF_6$, on heating, first, we observe one weak and broad signal related to the solid Li_3AlF_6. After 4-5 minutes, when the temperature is stabilized, we observe only a sharp signal corresponding to the melt. During the NMR experiments, the peaks do not change with time once the sample is liquid.

The HT spectra were recorded on Bruker AVANCE 400 (9.4 T) spectrometers using single pulse excitation consisting of 20 μs pulses; recycle delays of 500 ms, and 16 to 4096 scans to obtain a reliable signal-to-noise ratio. Several samples were checked after the HT NMR experiments using Solid-state NMR and X-ray diffraction. Solid-state NMR experiments were performed using Bruker Avance III spectrometer operating at 20.0 T, using a 4 mm resonance probe at a MAS frequency 14 kHz. ^{17}O and ^{27}Al MAS NMR data were collected from a single pulse experiment, with $\pi/12$ pulse widths between 1.0 μs and 1.2 μs and recycle delays of 0.5 s. The reported chemical shifts are referenced to 11 M solutions of $MgCl_2$, 1 M $Al(NO_3)_3$ for ^{25}Mg, ^{27}Al respectively, $CFCl_3$ for ^{19}F and tap water for ^{17}O. The NMR parameters (chemical shifts and line widths) were fitted by means of a DMfit program [30].

5.4. X-ray diffraction

X-ray diffraction analysis were done at room temperature under air on a Bruker D8 Advance diffractometer ($CuK\alpha_{1,2}$ radiation).

Acknowledgment

This study was financially supported by the Sacsess program (Grant Agreement number 323282). We thank Dr. E. Veron for X-ray measurements and Dr. F. Šimko for useful discussions.

References

[1] T. Fanghänel, J.-P. Glatz, R.J.M. Konings, V.V. Rondinella, J. Somers, Transuranium Elements in the Nuclear Fuel Cycle, in: D.G. Cacuci (Ed.) Handbook of Nuclear Engineering, Springer US, Boston, MA, 2010, pp. 2935−2998. https://doi.org/10.1007/978-0-387-98149-9_26.

[2] R. Ferrer, S. Bays, M. Pope, B. Forget, W. Skerjanc, M. Asgari, Summary Report on New Transmutation Analysis for the Evaluation of Homogeneous and Heterogeneous Options in Fast Reactors, 2008. http://dx.doi.org/10.2172/938446.

[3] J. Blomgren, S.K. Centrum, F. Karlsson, E. Aneheim, C. Ekberg, A. Fermvik, G. Skarnemark, J. Wallenius, J. Zakova, I. Grenthe, Partitioning and transmutation current developments–2010, A report from the Swedish, 2010.

[4] N. Ouvrier, H. Boussier, Recycling of MgO, Mo & ZrO_2 based Actinide-Bearing Matrices: Assessment of Reprocessing Feasibility & Waste Production, Procedia Chem. 7 (2012) 322−327. https://doi.org/10.1016/j.proche.2012.10.051.

[5] J.L. Holm, Thermodynamic properties of molten cryolite and other fluoride mixtures, Uden forlag, The University of Trondheim, NTH, Norway, 1971.

[6] B. Jenssen, Phase and Structure Relations for Some Alkali Aluminum Fluorides, Norges Tekniske Hgskole, Trondheim, NTH, Norway, 1969.

[7] J.L. Holm, B.J. Holm, Phase relations and thermodynamic properties in the ternary reciprocal system LiF-NaF-Na_3AlF_6-Li_3AlF_6, Thermochim. Acta 6 (1973) 375−398. http://dx.doi.org/10.1016/0040-6031(73)87005-4.

[8] S. Kašíková, M. Malinovský, L. Dobrovský, E. Linzer, Fázový diagram soustavy Li_3AlF_6-MgF_2. Sborník věd. prací Vys. školy báňské v Ostravě. Řada hutnická, 29(1) (1983) 93−99.

[9] K. Grjotheim, C. Krohn, M. Malinovský, K. Matiašovský, J. Thonstad, Aluminium electrolysis, Aluminium-Verlag, Düsseldorf, 1982.

[10] J.L. Holm, Ph.D. thesis, Technical University of Norway, Trondheim, 1963, pp. 210.

[11] A.A. Kostyukov, A.B. Karpov, Elektrometallurgija Tsvetnyh Metallov 188 (1956) 58−66.

[12] A.A. Kostyukov, N.Y. Anufrieva, Z.I. Balashova, Physico-chemical study of the system $NaF-AlF_3-CaF_2$ (MgF_2), Light Met. (1983) 389−396. http://dx.doi.org/10.1002/9781118359259.ch11.

[13] P. Fellner, K. Grjotheim, H. Kvande, Complex Formation in the Molten Systems NaF-MgF_2 and Na_3AlF_6-MgF_2, Acta Chem. Scand. 38a (1984) 699−702. http://dx.doi.org/10.3891/acta.chem.scand.38a-069.

[14] B. Gilbert, E. Robert, E. Tixhon, J.E. Olsen, T. Østvold, Structure and Thermodynamics of $NaF-AlF_3$ Melts with Addition of CaF_2 and MgF_2, Inorg. Chem. 35 (1996) 4198−4210. http://dx.doi.org/10.1021/ic951660l.

[15] Y. Hayakawa, H. Kido, The solubility of substances in molten salts. The determination of the solubility of metallic oxides in molten cryolite Science Reports of the Saitama Universityrsity, Series A. 1 (1952) 37−44.

[16] C. Bessada, V. Lacassagne, D. Massiot, P. Florian, J.P. Coutures, E. Robert, B. Gilbert, Structural and Dynamic Approaches of Molten Salts by High Temperature Spectroscopies, Z. Naturforsch. A 54 (1999) 162−166. http://dx.doi.org/10.1515/zna-1999-0212.

[17] C. Bessada, A. Rakhmatullin, A.-L. Rollet, D. Zanghi, Lanthanide and actinide speciation in molten fluorides: A structural approach by NMR and EXAFS spectroscopies, J. Nucl. Mater. 360 (2007) 43−48. http://dx.doi.org/10.1016/j.jnucmat.2006.08.012.

[18] V. Lacassagne, C. Bessada, P. Florian, S. Bouvet, B. Ollivier, J.-P. Coutures, D. Massiot, Structure of High-Temperature $NaF-AlF_3-Al_2O_3$ Melts: A Multinuclear NMR Study, The J. Phys. Chem. B 106 (2002) 1862−1868. http://dx.doi.org/10.1021/jp013114l.

[19] E. Robert, V. Lacassagne, C. Bessada, D. Massiot, B. Gilbert, J.P. Coutures, Study of $NaF-AlF_3$ Melts by High-Temperature ^{27}Al NMR Spectroscopy: Comparison with Results from Raman Spectroscopy, Inorg. Chem. 38 (1999) 214−217. http://dx.doi.org/10.1021/ic980677b.

[20] R.K. Harris, E.D. Becker, S. Cabral de Menezes, R. Goodfellow, P. Granger, NMR nomenclature. Nuclear spin properties and conventions for chemical shifts (IUPAC Recommendations 2001), Pure Appl. Chem. 73 (2001) 1679−1818. http://dx.doi.org/10.1351/pac200173111795.

[21] F. Tao, X.-J. Zhou, S.-F. Zhu, B.-J. Zhao, G.-Y. Hong, H.-P. You, Synthesis and Luminescence Characteristics of $LiMgAlF_6:Ln^{3+}$ (Ln = Ce, Eu, Tb), Cryst. Res. Tech. 32 (1997) 849−855. http://dx.doi.org/10.1002/crat.2170320618.

[22] L.A. O'Dell, S.L.P. Savin, A.V. Chadwick, M.E. Smith, A ^{27}Al MAS NMR study of a sol–gel produced alumina: Identification of the NMR parameters of the θ-Al_2O_3 transition alumina phase, Solid State Nucl. Magn. Reson. 31 (2007) 169−173. http://dx.doi.org/10.1016/j.ssnmr.2007.05.002.

[23] T.H. Walter, E. Oldfield, Magic angle spinning oxygen-17 NMR of aluminum oxides and hydroxides, J. Phys. Chem. 93 (1989) 6744-6751. http://dx.doi.org/10.1021/j100355a034.

[24] G. Moussaed, Apport de la RMN Haute température et de la Dynamique Moléculaire à l'étude de la fluoroacidité dans les fluorures fondus, Ph.D. thesis, Universite d'Orleans, Orleans, 2013, pp. 148−150.

[25] J.C.C. Freitas, M.E. Smith, Chapter 2 - Recent Advances in Solid-State ^{25}Mg NMR Spectroscopy, A.W. Graham (Ed.) Annu. Rep. NMR Spectrosc., Academic Press 2012, pp. 25−114. https://doi.org/10.1016/B978-0-12-397018-3.00002-8.

[26] G. Moussaed, V. Sarou-Kanian, M. Gobet, M. Salanne, C. Simon, A.L. Rollet, C. Bessada, Structure and Dynamics of Alkali and Alkaline Earth Molten Fluorides by High-Temperature NMR and Molecular Dynamics, in: Molten Salts Chemistry and Technology, John Wiley & Sons, Ltd, 2014, pp. 235−241. http://dx.doi.org/10.1002/9781118448847.ch4c.

[27] A. Sadoc, M. Body, C. Legein, M. Biswal, F. Fayon, X. Rocquefelte, F. Boucher, NMR parameters in alkali, alkaline earth and rare earth fluorides from first principle calculations, Phys. Chem. Chem. Phys. 13 (2011) 18539−18550. http://dx.doi.org/10.1039/C1CP21253B.

[28] G.L. Turner, S.E. Chung, E. Oldfield, Solid-state oxygen-17 nuclear magnetic resonance spectroscopic study of the group 11 oxides, J. Magn. Reson. 64 (1985) 316−324. https://doi.org/10.1016/0022-2364(85)90356-7.

[29] F. Claeyssens, J.M. Oliva, D. Sanchez-Portal, N.L. Allan, Ab initio predictions of ferroelectric ternary fluorides with the $LiNbO_3$ structure, Chem. Comm. (2003) 2440−2441. http://dx.doi.org/10.1039/B309000K.

[30] D. Massiot, F. Fayon, M. Capron, I. King, S. Le Calvé, B. Alonso, J.-O. Durand, B. Bujoli, Z. Gan, G. Hoatson, Modelling one- and two-dimensional solid-state NMR spectra, Magn. Reson. Chem. 40 (2002) 70−76. http://dx.doi.org/10.1002/mrc.984.

Graphical abstract: